attributed to so-called "charge resonance" excitations.[41b] Due to their inherent broadness, these transitions would probably be difficult to detect in $(CH)_x$ polarons, but the above-mentioned shifts induced in the local absorptions through interactions with neighboring $(CH)_x$ chains may constitute a factor which could thwart efforts to extrapolate oligomer data to the case of P^+/P^- in $(CH)_x$.

With the above caveat in mind, we can nevertheless say that our findings are not in contradiction with the assignment of a ~0.35-eV transient PA in $(CH)_x$ to polarons[14] (in fact, linear extrapolation of the oligomer E_2 energies leads very close to this energy). On the other hand, a 1.4-eV absorption[13] is difficult to reconcile with our results which indicate that the intense second transition (which is probably the only one which can be detected in transient PA experiments) should lie well below 1 eV, perhaps even below 0.5 eV, even if it is slightly shifted from the local transition in isolated $Pe^{\bullet+}$. Our findings therefore call for a reinterpretation of the results obtained by Yoshizawa et al.[13]

7. Summary

We have obtained electronic absorption spectra of polyene radical cations ($Pe^{\bullet+}$) with 3-13 conjugated double bonds capped by *tert*-butyl groups. These spectra are discussed within the framework of a simple MO/CI model which correctly predicts the occurrence of an intense high-energy and a weak low-energy electronic transition. Transient absorption spectra of carotenoid $Pe^{\bullet+}$ with 11-19 double bonds obtained previously by pulse radiolysis fit in very well with the present set of data except that a low-energy transition in these compounds had been missed in the earlier studies.

A linear extrapolation of E_1 and E_2 vs $1/n$ plots to infinite chain lengths leads to intercepts of ~0.4 eV (3200 cm^{-1}) for the intense second and ~0.1 eV (800 cm^{-1}) for the weak first electronic transition. The first of these values is in good agreement with the energy of a new band which was recently detected after photoexcitation of oriented all-trans polyacetylene[14] which suggests that an interpretation of this excitation in terms of polarons may be correct. In contrast, the assignment of a transient photoinduced absorption at 1.4 eV to polarons[13] appears questionable in view of the present results, in spite of the fact that the two experiments cannot be directly compared due to the presence of interchain interactions in polyacetylene.

MNDO calculations show that the ground-state electronic structure of $Pe^{\bullet+}$ (delocalization of spin and charge) changes only minimally as the chain length increases beyond ~0.5 double bonds which indicates that a linear extrapolation may not be valid in this case. In spite of this, the experimental $E_{1,2}$ vs $1/n$ plots show no deviation from linearity up to 19 double bonds which may be taken as evidence that spin and charge are less confined in $Pe^{\bullet+}$ excited states, in contrast to predictions from recent calculations.

8. Experimental Section

The *tert*-butyl-capped polyenes were synthesized at MIT according to the procedures outlined in ref 19. Since the samples with uneven numbers of double bonds were always mixtures of different rotamers, they were subjected to semipreparative HPLC on an analytical reversed-phase column prior to the spectroscopic measurements (C18 by Macherey Nagel, $CH_3CN(80)/H_2O(10)/CH_2Cl_2(5-10)$, 0.5-1 mL/min). In this way, the polyenes were rigorously purified and single rotamers could be significantly enriched in small but sufficient amounts.

The polyenes were dissolved to a concentration of $(2-5) \times 10^{-4}$ M in a 1:1 mixture of two Freons (CF_3Cl and CF_2Br-CF_2Br) and frozen to 77 K. After a reference spectrum was taken, the samples were exposed to ~0.5 Mrad of ^{60}Co γ-radiation whereupon the difference spectra (after minus before ionization) depicted in Figures 2 and 3 were obtained. For t-$BuPe^{\bullet+}$ with $n \leq 5$ it was possible to induce rotamerization by monochromatic photolysis as it had been observed before for the parent $Pe^{\bullet+}$. On the basis of this previous experience, we can say that in these cases the incipient $Pe^{\bullet+}$ was always the all-trans rotamer because it had the lowest $\lambda_{max}(D_2)$.

MNDO calculations were done with the VAMP program package[34] on a CONVEX C120 minisupercomputer.

Acknowledgment. This work is part of Project No. 20-28842.90 of the Swiss National Science Foundation, and at MIT was supported by the Office of Basic Energy Research, Office of Basic Energy Sciences, Chemical Sciences Division of the U. S. Department of Energy (Contract DE-FG02-86ER13564). We thank our colleagues D. Baeriswyl (University of Fribourg), J. Frommer (IBM Almaden), R. Silbey (MIT), and B. Kohler (University of California, Riverside) for invaluable advice and comments and Prof. E. Haselbach for continuing support and encouragement.

η_2 versus η_1 Coordination of Aldehydes and Ketones in Organometallic Complexes. A Semiempirical Theoretical Study

Françoise Delbecq* and Philippe Sautet

Contribution from the Institut de Recherche sur la Catalyse, 2 avenue Einstein, 69626 Villeurbanne Cedex, France, and Ecole Normale Supérieure de Lyon, 46 allée d'Italie, 69364 Lyon Cedex 07, France. *Received February 28, 1991*

Abstract: The η_1 and η_2 coordinations of aldehydes and ketones on several types of organometallic fragments have been compared on the basis of an extended Hückel molecular orbital analysis. The electronic description of the interaction between the organic ligand and the metallic part leads to the distinction between stabilizing two electron interactions and destabilizing four electron ones. The stabilizing interactions concern the frontier orbitals, oxygen lone pair with the LUMO of the metallic fragment for the η_1 mode, and π^*_{CO} with occupied d for the η_2 mode and always favor the η_2 coordination. However, four electron interactions between low-lying orbitals play an important role in the determination of the preferred structure. These interactions result from an indirect coupling through the metal center between occupied orbitals of the organic molecule and those of other ligands on the complex. For overlap reasons these ligand-ligand "through-bond" interactions are stronger for the η_2 mode, thus making this structure less energetically favored. The balance between these two conflicting electronic effects is described for various metals, ligand environments, and substituents on the organic molecule. On this basis, the behavior of d^{10} ML_2, d^8 ML_3, d^6 ML_5, and $CpML_2$ type fragments is detailed. We show how the preferred coordination can be changed for a given type of organometallic fragment by a modification of ligands or substituents.

I. Introduction

Over the past decade, there have been numerous experimental results regarding organometallic complexes having aldehydes and ketones as ligands. Most of them have been isolated and characterized by X-ray spectroscopy, while the others have been analyzed only by IR spectroscopy (for a review see footnote 1 and

0002-7863/92/1514-2446$03.00/0

Scheme I

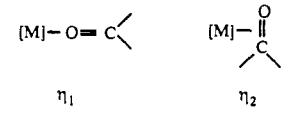

η_1 η_2

references herein). Two modes of coordination appear. In the first one, the organic carbonyl compound coordinates via the oxygen atom (η_1 coordination). In the second one, the coordination takes place through the π_{CO} bond (η_2 coordination). Both coordination modes are shown in Scheme I, where [M] is an organometallic fragment.

The experiments demonstrate that the organometallic fragments fall into two classes: when the metallic part [M] is a d^{10} ML_2 fragment ($Pt(PR_3)_2$,[2] $Pd(PR_3)_2$,[3] $Ni(PR_3)_2$[4]) or a C_{2v} d^8 ML_4 fragment ($Os(CO)_2(PR_3)_2$,[5] $Ru(CO)_2(PR_3)_2$,[6] $Fe(CO)_2(PR_3)_2$[7]), the η_2 form is preferred; when [M] is a d^8 ML_3 fragment ($PtCl_2$(pyridine),[8a] $Pt^+CH_3(PR_3)_2$[8b]), an octahedral d^6 ML_5 fragment ($RuCOCl(PR_3)_2$ $SnCl_3$,[9] $Mn_2(CO)_9$[10]), or a d^6 $CpML_2$ fragment ($CpFe^+(CO)_2$[11]), the η_1 form is preferred (Cp = cyclopentadienyl). Nevertheless, some exceptions occur: for the d^6 ML_5 $Os(NH_3)_5^{2+}$ fragment, the coordination is η_2[12] and, in the case of the d^6 $CpRe^+NO(PR_3)$ fragment, the coordination is η_1 for ketones[13] and η_2 for aldehydes[14a] as in the case of $CpRe(CO)_2$.[14b] In such complexes, the two forms can coexist with a η_2/η_1 ratio depending on the substituents.[14c]

The purpose of this work is to explain these trends and to bring out the electronic factors which control the coordination toward the η_1 or the η_2 form. The method used is based on extended Hückel calculations. A more quantitative ab initio study will appear in the near future. To our knowledge, only a few theoretical results have been published on complexes having aldehydes or ketones as ligands, and those concern ab initio studies on $Ni(PH_3)_2(H_2CO)$,[15] $Fe(CO)_{4-n}(PH_3)_n(R_2CO)$ (R = H or CH_3),[16] and $Co(CO)_3H(H_2CO)$.[17] The advantage of the extended Hückel method is that a large number of structures can be calculated,

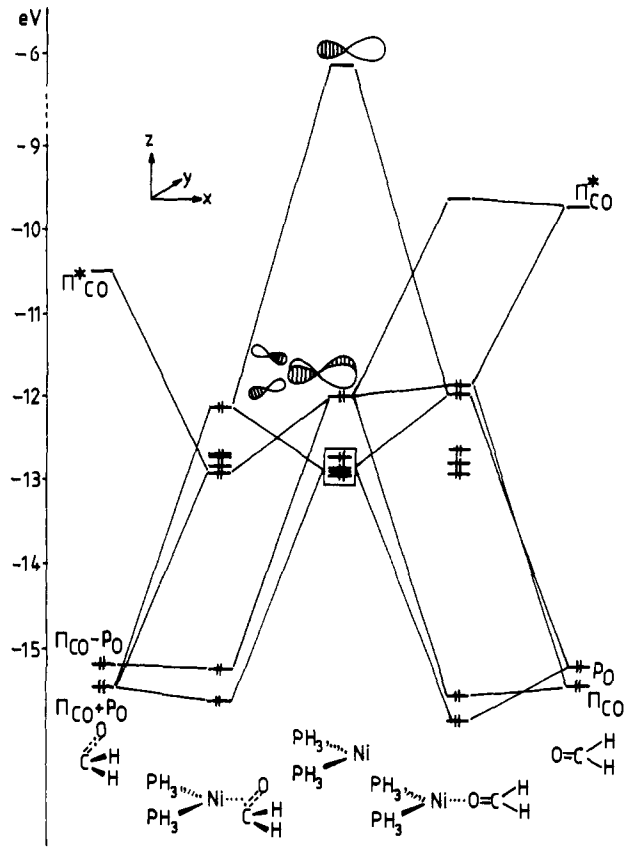

Figure 1. Orbital interaction diagram between the d^{10} $Ni(PH_3)_2$ fragment and H_2CO in the η_1 form (on the right) and in the η_2 form (on the left).

thus allowing numerous variations in the metal, ligands, and organic substituents. As a result, the trends in the experimental results may be qualitatively analyzed.

The two classes of complexes distinguished on an experimental basis belong to the same isolobal group, as both d^{10} ML_2 and d^8 ML_3 are isolobal to CH_2.[18] Thus it is necessary to go beyond isolobal analysis to understand the different behavior of complexes with aldehyde fragments. As a matter of fact, the two linkages of the organic carbonyl compound have a very different electronic structure. For the η_1 coordination, the OCR_2 fragment is an electron donor through oxygen lone pair electrons (σ_O), and so good electron-withdrawing capabilities of the metallic fragment are required to stabilize this form. On the other hand, the η_2 lateral coordination mainly occurs with the π electrons, and we will show that the back-bonding interaction (with π^*_{CO}), involving the Lewis basis capability of the metallic fragment, is the major component of this interaction. Then, it is not only the topological shape and symmetry of the metal frontier orbitals which are important, but also their energetic position with respect to the σ_O and π^*_{CO} orbitals.

The two types of frontier orbital interactions will be described in section II using a characteristic example within each class built from the same Ni atom: the d^{10} $Ni(PH_3)_2$ fragment for the η_2 class, and the d^8 $NiCl_2(PH_3)$ fragment for the η_1 class. The origin of their different electronic properties with respect to aldehyde coordination will be underlined.

However, this frontier orbital analysis will not provide a complete understanding of these species. Indeed, in these complexes, ligand–ligand through metal interactions can play an important role. These destabilizing "four-electron" interactions involve low-lying ligand orbitals which are rarely included in the theoretical analysis. They are not equivalent to the classical four-electron steric interactions since the ligand orbitals involved have

(1) Huang, Y. H.; Gladyzs, J. A. *J. Chem. Educ.* **1988**, *65*, 298.
(2) (a) Carke, B.; Green, M.; Osborn, R. B. L.; Stone, F. G. A. *J. Chem. Soc. A* **1968**, 167. (b) Head, R. A. *J. Chem. Soc., Dalton Trans.* **1982**, 1637.
(3) Empsall, H. D.; Green, M.; Stone, F. G. A. *J. Chem. Soc., Dalton Trans.* **1972**, 96.
(4) (a) Countryman, R.; Penfold, B. R. *J. Cryst. Mol. Struct.* **1972**, *2*, 281. (b) Tsou, T. T.; Huffman, J. C.; Kochi, J. K. *Inorg. Chem.* **1979**, *18*, 2311. (c) Kaiser, J.; Sieler, J.; Walther, D.; Dinjus, E.; Golic, L. *Acta Cryst.* **1982**, *B38*, 1584.
(5) Clark, G. R.; Headford, C. E. L.; Marsden, K.; Roper, W. R. *J. Organomet. Chem.* **1982**, *231*, 335.
(6) (a) Cooke, M.; Green, M. *J. Chem. Soc. A* **1969**, 651. (b) Burt, R.; Cooke, M.; Green, M. *J. Chem. Soc. A* **1970**, 2975.
(7) Berke, H.; Huttner, G.; Weiler, G.; Zsolnai, L. *J. Organomet. Chem.* **1981**, *219*, 353.
(8) (a) Courtot, P.; Pichon, R.; Salaun, J. Y. *J. Organomet. Chem.* **1985**, *286*, C17. Auffret, J.; Courtot, P.; Pichon, R.; Salaun, J. Y. *J. Chem. Soc., Dalton Trans.* **1987**, 1687. (b) Thayer, A. G.; Payne, N. C. *Acta Crystallogr.* **1986**, *C42*, 1302.
(9) Gould, R. O.; Sime, W. J.; Stephenson, T. A. *J. Chem. Soc., Dalton Trans.* **1978**, 76.
(10) Bullock, R. M.; Rappoli, B. J.; Samsel, E. G.; Rheingold, A. L. *J. Chem. Soc., Chem. Commun.* **1989**, 261.
(11) (a) Williams, W. E.; Lalor, F. J. *J. Chem. Soc., Dalton Trans.* **1973**, 1329. (b) Foxman, B. M.; Klemarczyk, P. T.; Liptrot, R. E.; Rosenblum, M. *J. Organomet. Chem.* **1980**, *187*, 253.
(12) (a) Harman, W. D.; Fairlie, D. P.; Taube, H. *J. Am. Chem. Soc.* **1986**, *108*, 8223. (b) Harman, W. D.; Sekine, M.; Taube, H. *J. Am. Chem. Soc.* **1988**, *110*, 2439.
(13) Dalton, D. M.; Fernandez, J. M.; Emerson, K.; Larsen, R. D.; Arif, A. M.; Gladysz, J. A. *J. Am. Chem. Soc.* **1990**, *112*, 9198.
(14) (a) Garner, C. M.; Quiros Mendez, N.; Kowalczyk, J. J.; Fernandez, J. M.; Emerson, K.; Larsen, R. D.; Gladysz, J. A. *J. Am. Chem. Soc.* **1990**, *112*, 5146. Buhro, W. E.; Georgiou, S.; Fernandez, J. M.; Patton, A. T.; Strouse, C. E.; Gladysz, J. A. *Organometallics* **1986**, *5*, 956. (b) Berke, H.; Birk, R.; Huttner, G.; Zsolnai, L. *Z. Naturforsch.* **1984**, *39B*, 1380. (c) Quiros Mendez, N.; Arif, A. M.; Gladysz, J. A. *Angew. Chem., Int. Ed. Engl.* **1990**, *29*, 1473.
(15) Sakaki, S.; Kitaura, K.; Morokuma, K.; Ohkubo, K. *Inorg. Chem.* **1983**, *22*, 104.
(16) (a) Rosi, M.; Sgamellotti, A.; Tarantelli, F.; Floriani, C.; Guest, M. F. *J. Chem. Soc., Dalton Trans.* **1988**, 321. (b) Rosi, M.; Sgamellotti, A.; Tarantelli, F.; Floriani, C. *Inorg. Chem.* **1988**, *27*, 69.
(17) Versluis, L.; Ziegler, T. *J. Am. Chem. Soc.* **1990**, *112*, 6763.
(18) (a) Hoffmann, R. *Angew. Chem., Int. Ed. Engl.* **1982**, *21*, 711. (b) Albright, T. A. *Tetrahedron* **1982**, *38*, 1339.

a small through-space overlap and interact mainly by the intermediate of the metal atom. This is therefore distinct from those arguments involving steric hindrances. In section III we shall discuss this through-bond interaction for the two previously described fragments and for the $Fe(CO)_2(PH_3)_2(H_2CO)$ complex. We will show that it generally favors the η_1 interaction.

This analysis will be extended in section IV to other ligands and to C_{2v} d^8 ML_4 and d^6 ML_5 organometallic fragments in order to include in the discussion the other types of aldehydes and ketones complexes. Fragments with cyclopentadienyl (Cp) ligands will also be considered.

II. Frontier Orbital Interaction Analysis

1. The $Ni(PH_3)_2(H_2CO)$ Complex. With the classical substitution of the PR_3 ligands by PH_3 groups, this complex is a model of the experimental $Ni(PR_3)_2(R_2CO)$ complex, whose geometry has been determined by X-ray analysis as belonging to the η_2-coordination class. Let us describe the frontier orbital interaction for this complex (**1a**) and for the hypothetical η_1 conformation (**1b**). The geometrical description of both complexes, and of all of those studied in the following, is detailed in Appendix II.

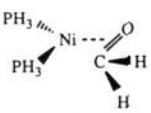

(1a)

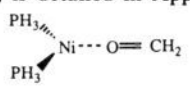

(1b)

The valence orbitals of the d^{10} C_{2v} ML_2 organometallic fragment[18b] are shown in Figure 1. After a set of four (3 + 1) nonbonding (or closely) metal d orbitals, the main features of this diagram are the high HOMO of mainly d_{xy} character with significant antibonding mixing with the L ligands and the s–p hybrid LUMO. Both orbitals point in the opposite direction of the L ligands and are therefore optimal for the interaction with the (H_2CO) fragment.

In the case of the η_2 coordination (**1a**), the interaction diagram (Figure 1) resembles the well-known one of the $ML_2(C_2H_4)$ complex.[19] The H_2CO fragment is strongly hybridized toward sp^3 in this case (see Appendix II). Therefore, mixing occurs between the π and σ orbitals of the planar molecule. If a π^*_{CO}-type orbital can still be recognized, π_{CO} mixes with the p_y lone pair, leading to the two combinations shown below.

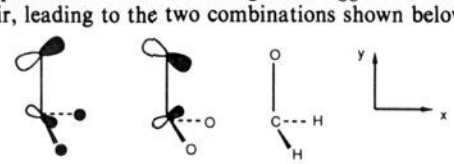

$\pi_{CO} + P_O$ $\pi_{CO} - P_O$

The main stabilizing interaction is between the low vacant π^*_{CO} and the high HOMO of the metallic fragment, yielding an important back-bonding electron transfer. On the contrary, the interactions between the occupied orbitals of H_2CO and the high LUMO of the ML_2 group are rather weak. Only π_{CO} has a significant overlap, but it lies quite low in energy because of the electronegativity of oxygen. So, in this η_2 case, interaction is dominated by back-bonding. This is in complete agreement with SCF ab initio calculations on the same complex.[15] The weakness of the σ-donative interaction of the classic Chatt–Dewar–Duncanson model has also been found in ab initio calculations on iron complexes[16] with H_2CO.

Things are different for the η_1 isomer. The interaction with π^*_{CO} is much weaker, since the overlap with this orbital, which has the main component on the carbon atom, is small. By contrast, the p_x lone pair of oxygen is now in good position in terms of overlap viewpoint for a dative interaction with the sp LUMO of the metallic fragment. This interaction is not very strong because of the big energy difference between these levels. Nevertheless, the interaction is dominated by this dative interaction. It should be pointed out that the choice of the symmetrical linear conformation versus the bent experimental one (see Appendix II) simplifies the interaction diagram without modifying it significantly. This symmetric choice, which is the extended Hückel energy minimum, only yields a very small change in total energy compared to the bent case. This choice also avoids some complicated orbital mixings and allows a more simple equivalent interpretation of the electronic interaction.

Therefore, the η_1 and η_2 conformations are associated with different types of bonding with the ML_2 group. The $Ni(PH_3)_2$ fragment, which is a Lewis basis, is well suited for the η_2 conformation since in this case the population of π^*_{CO} by metal electrons is the main process. On the contrary, being a poor electron acceptor, it is unfavorable to the η_1 coupling (see Tables I and II).

2. Effect of Substituents on the Aldehyde: $Ni(PH_3)_2(R_2CO)$. Experimental results indicate that the most common ligands which coordinate in the η_2 mode are the aldehydes and the substituted ketones such as $(CF_3)_2CO$ or Ph_2CO. Only a few η_2 complexes involving acetone $(CH_3)_2CO$ have been described.[12,20] In the following we will explain this fact. The η_1 and η_2 complexes of acetone (R = CH_3) and hexafluoroacetone (R = CF_3) have been studied as **1a** and **1b**.

The first column of Table I describes the energy difference Δ between the η_1 and the η_2 forms for the various substituents. Notice that the η_2 form is the most stable one, as indicated by the positive values in the table, following then the previous qualitative argument and in agreement with the SCF ab initio result.[15] It should be pointed out that, for acetone, Δ is noticeably smaller than for formaldehyde or hexafluoroacetone. The method used does not allow too much emphasis to be placed on quantitative values. Nevertheless, we can conclude that acetone has a smaller tendency to give η_2 complexes than formaldehyde or hexafluoroacetone. The effect of substituting the hydrogens by methyls in H_2CO is to shift up all the interesting orbitals (p_{xO}, π_{CO}, and π^*_{CO}). Those orbitals become somewhat delocalized over the methyl groups and their overlap with the metallic part is reduced. For the η_1 form, the two effects cancel; the better interaction with the metallic LUMO that results from the raising of the oxygen lone-pair is balanced by the smaller overlap. For the η_2 form, on the contrary, the two effects add and diminish the interaction between π^*_{CO} and the metallic HOMO.

The calculated binding energies are shown in Table II. The positive values mean that the aldehyde or ketone is not bound to

Table I. Energy Difference Δ (kcal/mol) between the η_1 and the η_2 Forms of the Complexes $M(PH_3)_2R_2CO$[a]

metal	Ni	Pd	Pt
H_2CO	15.6	19.6	16.1
$(CH_3)_2CO$	3.9	9.6	5.7
$(CF_3)_2CO$	11.0	17.1	11

[a] A positive value means that the η_2 form is the more stable.

Table II. Energy Components (kcal/mol)[a] for Interaction between $M(PH_3)_2$ and R_2CO[b]

		η_1 form	η_2 form		
R_2CO	M	INT = BE	DEF	INT	BE
H_2CO	Ni	5.4	13.7	−23.9	−10.2
	Pd	−2.1	13.7	−35.4	−21.7
	Pt	−6.4	13.7	−36.4	−22.7
$(CH_3)_2CO$	Ni	6.8	13.8	−10.9	2.9
	Pd	−1	13.8	−24.4	−10.6
	Pt	−5.1	13.8	−24.7	−10.9
$(CF_3)_2CO$	Ni	5.9	12	−17.1	−5.1
	Pd	−1.2	12	−30.2	−18.3
	Pt	−6.1	12	−29.2	−17.2

[a] A negative (positive) energy designates stabilization (destabilization). [b] INT = interaction energy, DEF = deformation energy, BE = binding energy.

(19) Albright, T. A.; Hoffmann, R.; Thibeault, J. C.; Thorn, D. L. *J. Am. Chem. Soc.* **1979**, *101*, 3801.

(20) Wood, C. D.; Schrock, R. R. *J. Am. Chem. Soc.* **1979**, *101*, 5421.

the metallic fragment. In the case of the η_2 form, the binding energy has been decomposed in a deformation energy component DEF for the R_2CO ligand (always positive) and the electronic interaction energy INT between the deformed ligand and the metallic fragment (BE = INT + DEF). As discussed above, the interaction energies INT are identical in the η_1 form for H_2CO and acetone, whereas INT is much smaller for acetone than formaldehyde in the η_2 coordination. We notice that the deformation energies DEF are equivalent for the three considered ligands while acetone shows a marked decrease in the interaction energy, resulting in a positive (unstable) binding energy. This result is in contrast with SCF ab initio calculations,[16] where the decrease in binding energy for acetone is also found but attributed to a strong increase in the positive deformation energy with nearly no variation in the interaction energy. Nevertheless, except for the energy decomposition, the qualitative difference between formaldehyde and acetone ligand is in agreement with our results.

The substitution by the electron-withdrawing CF_3 groups lowers the orbital energies relative to the CH_3 groups and diminishes the orbital delocalization. As a result, hexafluoroacetone has an intermediate behavior between formaldehyde and acetone (see Tables I and II). In fact, the electron-withdrawing character of CF_3 is not sufficiently well described at the EHT level. Ab initio calculations on the isolated R_2CO with the 3-21G basis set (MONSTERGAUSS program[21]) show that the orbitals of hexafluoroacetone are lower than those of formaldehyde. Therefore, the η_2 coordination of hexafluoroacetone must be even more favorable than that of formaldehyde. This explains why this ketone is often used as ligand.

In conclusion, the study of the substituent effect explains why complexes of $Ni(PH_3)_2$ with acetone, either η_1 or η_2, do not exist, and why electron-withdrawing substituents on ketones allow complexation in the η_2 form.

3. Influence of the Metal Nature. The results obtained by changing the nature of the metal atom along the Ni, Pd, Pt series are also given in Tables I and II. If we consider first the η_2 coordination of the aldehyde, we see that Pd gives a significant increase in binding energy. This is explained by the higher position of the d orbitals in Pd as compared to Ni, thus yielding a better interaction with the π^*_{CO} and consequently a higher electron transfer toward this orbital. The binding energy difference between Pd and Pt is much smaller. The d orbitals of platinum are at a slightly lower energy, producing a small decrease in back-bonding, balanced by an increase in the bonding interaction between π_{CO} and the metallic LUMO.

If the η_1 coordination is now considered, the binding energy variations associated with a change in the metal atom cannot be directly linked to the two-electron interaction between the oxygen lone pair and metal LUMO. Secondary four-electron interactions between d block and R_2CO occupied orbitals also play a role and are also modified along the Ni, Pd, Pt series. However, the η_1 and η_2 binding energy variations are roughly parallel so that the energy difference Δ is not strongly modified.

The η_2 preferred coordination is an intrinsic property of the electron donor d^{10} ML_2 fragment. Reversing the coordination preference can be achieved by varying the ligand field around the Ni atom in order to diminish the donor capability of the metallic fragment or to increase its acceptor character as it will be described in the following section.

4. The $NiCl_2(PH_3)(H_2CO)$ Complex. The $NiCl_2(PH_3)$ group is a d^8 C_{2v} ML_3 fragment. The valence orbitals shown in Figure 2 are very different from those of the d^{10} ML_2 fragment. Because of the removal of two electrons, the LUMO has now a main d component, with metal s and p mixing yielding a hybridization away from the L ligands. This LUMO of spd character is low in energy. The d_{xy} orbital is no longer d–L antibonding and lies at the same energy as the other occupied orbitals. Furthermore, it is no longer hybridized toward the empty site. Therefore, this organometallic fragment with both a lower LUMO and d_{xy} orbital

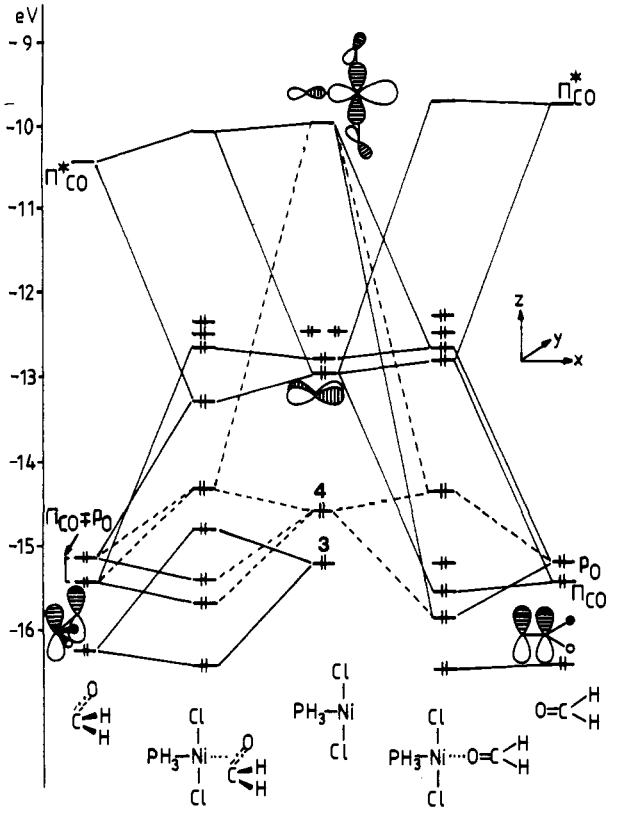

Figure 2. Orbital interaction diagram between the d^8 $NiCl_2(PH_3)$ fragment and H_2CO in the η_1 form (on the right) and in the η_2 form (on the left). Orbitals **3** and **4** are drawn in the text.

should present better withdrawing and poorer donor capabilities.

This is clearly apparent in the interaction diagram of Figure 2 where the η_2 and η_1 interactions are both described, similarly to Figure 1 for the $Ni(PH_3)_2$ fragment. For the η_2 coordination (**2a**), compared to the ML_2 case, the lower energy of d_{xy} and the lack of any hybridization toward the H_2CO ligand lead to a diminished back-bonding interaction with the π^*_{CO} orbital.

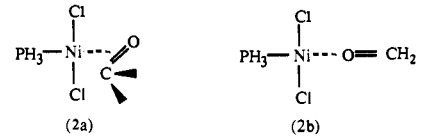

If we consider now the η_1 interaction (**2b**), dominated as before by the σ-donation from p_{xO} lone pair into the LUMO of the complex, differences are small. One could have expected an increase of this interaction due to the lower position of the LUMO. In this case, the overlap criterion yields a reverse effect, since the LUMO is now mainly of d character, compared to sp for the ML_2 case, and d orbitals generally give lower overlap than s and p ones.

We can then conclude that the d^8 ML_3 fragment is less donor than d^{10} ML_2 and is therefore less favorable for the η_2-coordination mode, as far as the interaction between frontier orbitals is concerned. However, this simple frontier orbital analysis is not sufficient for a complete understanding of the change in coordination of H_2CO between $Ni(PH_3)_2$ and $Ni(Cl)_2$ PH_3 fragments.

Now indirect interactions between orbitals of H_2CO and of the other ligands on the metal center must also be included for a more precise description of the electronic interaction.

III. Ligand–Ligand through Metal Interaction as a Second Factor for Coordination Preference.

1. A Decomposition of the Binding Energy. In order to understand precisely the coordination difference of H_2CO on the two organometallic fragments of section II, d^{10} $Ni(PH_3)_2$ and d^8 $NiCl_2(PH_3)$, a decomposition of the binding energy BE on each molecular orbital of the two interacting moieties has been performed. Within a fragment molecular orbital (FMO) approach,

(21) Peterson, M.; Poirier, R. *MONSTERGAUSS*; Chemistry Department, University of Toronto: Toronto, Canada, June 1981.

Table III. Decomposition of the Binding Energy in "d + H_2CO" and "Ligands" Contributions (see text).

	$Ni(PH_3)_2$		$Ni(PH_3)Cl_2$		$Fe(CO)_2(PH_3)_2$	
	η_1	η_2	η_1	η_2	η_1	η_2
A. Absolute Energies						
d + H_2CO	9	−12	−29	−29	3	−17
ligand	−3	2	13	28	−3	9
total	6	−10	−16	−1	0	−8
B. Relative to the Lowest Energy in Each Case						
d + H_2CO	21	0	0	0	20	0
ligand	0	5	0	15	0	12
total	16	0	0	15	8	0

each molecular orbital of the total complex has been associated with the FMO of either H_2CO or the metallic fragment that represents the dominant contribution in this orbital. This allows an unambiguous one to one assignment between each MO of the complex and a FMO of the two fragments. For each occupied MO, an individual contribution to the binding energy was then simply calculated as the difference between the energies of this MO and of the associated FMO. Obviously, the addition of these individual contributions on all occupied orbitals yields exactly the calculated binding energy. These individual energy contributions have been partially recombined into three groups of occupied orbitals: the orbitals of mainly metal d character, the molecular orbitals originating from the H_2CO fragment, and those centered on the other ligands that will be singly labeled as "ligands" in the following.

The addition of "d" and "H_2CO" contributions is the fraction of the binding energy that only deals with the interaction of H_2CO with the metal-centered orbitals of the organometallic fragment. This d + H_2CO contribution reduces mainly to the two-electron frontier orbital interactions previously described. By contrast, the "ligands" contribution indicates how the other ligands on the fragment are disturbed by further complexation of H_2CO. This contribution is largely due to four-electron interactions and is therefore destabilizing.

The decomposition in the case of $Ni(PH_3)_2$ and $NiCl_2(PH_3)$ is shown in Table III. In the case of $Ni(PH_3)_2$, the ligand contribution is weak and the preferred coordination is then fully controlled by the frontier orbital interactions. This is not at all the case for the d^8 $Ni(PH_3)Cl_2$ complex, where d + H_2CO contributions are nearly equal for the η_1 and the η_2 forms and where the difference in total energy only comes from the ligand contribution. In this case, the η_2 coordination is no longer favored by frontier orbitals as compared to $Ni(PH_3)_2$, and the interactions of H_2CO with other ligands determine the preferred coordination mode.

2. The Ligand–Ligand Interactions. In the case of $NiCl_2(PH_3)$, the ligand contribution to the binding energy is strongly destabilizing and this interaction between H_2CO and other ligand orbitals can be mainly described by a 4e repulsive interaction. However, this destabilizing interaction is not a direct steric repulsion. More precisely, this interaction does not come from a direct overlap of occupied orbitals of H_2CO and ligands, but rather from an indirect through-bond[22] coupling between these orbitals mediated by the metal d orbitals.

In the organometallic fragment $NiCl_2(PH_3)$, the Cl p_x orbitals are coupled in a bonding way with metal d_{xy} (**3**). In the resulting

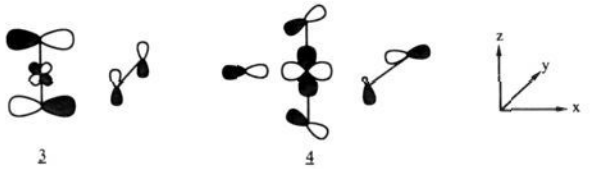

3 4

occupied orbital, the d component is small but significant. The low-lying p_z occupied orbital of the incoming H_2CO will thus overlap with this d component and a 4e destabilization follows. This destabilization is stronger in the lateral η_2 coordination (the overlap in the η_1 coordination is smaller by a factor of 3). In the same way, another low-lying occupied orbital (**4**), bonding with the three ligands and having a nonnegligible d component, overlaps with the p_{xO} lone pair in the η_1 form and with the π_{CO} orbital in the η_2 form. A 4e destabilization results with about the same strength in both coordinations.

These interactions are not the only 4e interactions involved, but they are the most significant. Consequently, the preferred coordination mode is controlled by the former ligand–ligand 4e interaction (**3**). The frontier orbital arguments described in section II cannot reverse the tendency in that case and only have a quantitative influence. Therefore, the η_1 coordination mode is always preferred whatever the metal (Ni, Pd, or Pt) for $MCl_2(PH_3)(R_2CO)$ complexes (Table IV). As previously explained, it is more preferred for acetone than formaldehyde. If the effect of the nature of the metal is concerned, the trends are more easily understood than for $Ni(PH_3)_2(R_2CO)$. This time the LUMO of the metallic fragment has mainly d character, and the position of the s–p orbital does not intervene much. Therefore, the higher the d orbitals (e.g., Pd compared to Ni), the less favored the η_1 form with respect to the η_2 one without being able to reverse the η_1 preference imposed by the 4e interaction.

Table IV. Energy Difference Δ (kcal/mol) between the η_1 and η_2 Forms of the Complexes $MCl_2PH_3(R_2CO)$[a]

metal	Ni	Pd	Pt
H_2CO	−14.9	−1.4	−8.7
$(CH_3)_2CO$	−46.0	−25.3	−32.9

[a] A negative value means that the η_1 form is more stable.

3. The $Fe(CO)_2(PH_3)_2(H_2CO)$ Complex. This complex is interesting in that it behaves like $Ni(PH_3)_2(H_2CO)$ for the frontier orbital interactions and like $NiCl_2(PH_3)(H_2CO)$ for the ligand–ligand interactions. As before, both coordination modes **5a** and **5b** have been studied. **5a** is known experimentally.

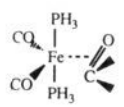

5a

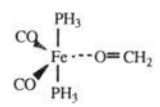

5b

The same decomposition of the binding energy as before has been performed for the interaction of H_2CO with the d^8 C_{2v} ML_4 fragment $Fe(CO)_2(PH_3)_2$. The results shown in Table III (bottom) indicate that the 4e ligand–ligand interactions are important (as in the ML_3 case) but not sufficient to prevail over the frontier orbital interactions.

Examination of the diagrams in Figure 3 provides some insight to these results. The frontier orbitals of the d^8 ML_4 fragment are similar to those of the d^{10} ML_2 fragment previously described. Therefore, the frontier orbital interactions are identical. Nevertheless, the LUMO of the d^8 ML_4 fragment is much lower than the LUMO of the d^{10} ML_2 fragment. Since only four d orbitals are occupied, the LUMO of the d^8 ML_4 fragment is mainly a d orbital hybridized by p_x instead of being a sp orbital as in d^{10} ML_2. Consequently, the interaction of the LUMO of both p_{xO} in the η_1 form and π_{CO} in the η_2 form is much stronger than in the ML_2 case (see Table III, top). The binding energies are better in both coordination modes, but their difference is the same as for the ML_2 case.

As in complex **2a** $NiCl_2(PH_3)(\eta_2\text{-}H_2CO)$, two axial ligands exist in **5a**, perpendicular to the C=O bond, and a similar 4e ligand–ligand interaction ensues between the p_z orbital of CH_2O and two occupied orbitals **6** and **7** of $Fe(CO)_2(PH_3)_2$. These orbitals result from the interaction of the Fe–P bonds with the π_{CO} orbitals of the CO ligands. These 4e interactions are similar in magnitude to the interaction of the p_z orbital of CH_2O with **3**.

Owing to the lack of ligand on the x axis, an orbital looking like **4** no longer exists, and the corresponding 4e destabilizing

(22) Hoffmann, R. *Acc. Chem. Res.* **1971**, *4*, 1.

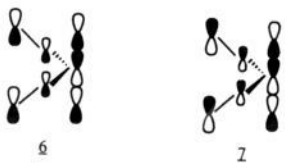

6 7

interaction mentioned in complex $NiCl_2(PH_3)(H_2CO)$ is suppressed. In this case the ligand–ligand interactions with the d^8 ML_4 fragment are much smaller than with the d^8 ML_3 one (Table III, top) and are not sufficient to reverse the situation. The 2e interactions dominate and favor the η_2 form in agreement with the experimental data. However, the energy difference with the η_1 form is less than for the ML_2 case (see Table V, column 1). As previously, the substitution of the organic part and the metal nature have been studied. Similar to the ML_3 case, all interacting orbitals have mainly d character. The same reasoning as above explains why the η_2 form is more favored for ruthenium than for iron since its d orbitals are higher.

The experimental complex of osmium $Os(CO)_2(PH_3)_2(H_2CO)$[5] has also been calculated. Osmium is a more electropositive metal than ruthenium and effectively the η_2 form is more stable by 36.3 kcal/mol. This indicates that the back-donation in the π^*_{CO} is very strong. Effectively the C=O overlap population becomes 0.65 instead of 0.82 in H_2CO alone and 0.74 in $Ni(PH_3)_2(H_2CO)$. This explains why experimental results have found the CO bond to be unusually long (1.57 Å) instead of 1.32 Å as in the usual formaldehyde complexes.

The results obtained for $(CF_3)_2CO$ could seem surprising since both on Fe and Ru the η_2 form is more preferred for acetone than hexafluoroacetone (for comparison, see Table I). In fact, in complexes where the ligand–ligand interactions exist, these destabilizing interactions increase with the substitution on the organic part. Therefore, the ligand–ligand interactions are stronger with $(CF_3)_2CO$ than with $(CH_3)_2CO$, explaining why the situation is inverted relative to the case of $Ni(PH_3)_2$.

In conclusion, we have shown that, in some complexes, four-electron ligand–ligand destabilizing interactions play an important role and can prevail over the two-electron frontier orbital stabilization in the determination of the preferred coordination mode.

IV. Extension to Various Complexes

The preceding sections have pointed out the main interactions accountable for the η_1 or η_2 coordination. The η_1 coordination is controlled by the oxygen lone-pair–metal vacant orbital interaction and the η_2 coordination by the balance between the stabilizing π^*_{CO}–metal occupied orbital interactions and the destabilizing four-electron ligand–ligand interactions. We will see in this section how to modify the relative importance of these three interaction types in order to favor one form over the other.

1. Influence of the Position and Nature of the Ligands. A ligand which destabilizes the d_{xy} occupied orbital interacting with π^*_{CO} will increase this interaction and thus favor the η_2 form and vice versa. A ligand which stabilizes the LUMO interacting with the oxygen lone pair will increase this interaction and thus favor the η_1 form. The ligand nature modifies also the shape and energy of the low-lying occupied orbitals (called z) responsible for the 4e-destabilizing interactions.

1.1. Nature of the Phosphine Ligands in $ML_2(R_2CO)$ Complexes. When the model PH_3 ligand is replaced by the experimental PR_3 one (R = CH_3 of Ph, for example) which is a better σ-donor, both the d_{xy} orbital and the s–p LUMO are shifted up. However, the shift is not too strong because the lone pair of phosphorus is somewhat more delocalized on R in PR_3 than in PH_3. Therefore, the associated decrease in the orbital overlap between the PR_3 lone pair and the metal counterbalances the important energy difference between the PH_3 and PR_3 lone pairs. As a consequence, the η_1 form is less favored by 1–3 kcal/mol, and the η_2 form is more favored by roughly the same value, so that the difference Δ is increased by 3–5 kcal/mol. The trends of Tables I and II are not modified. For example, the calculations for $Ni(PMe_3)_2(H_2CO)$ give BE = 6.7 and −12.4 kcal/mol in the η_1 and η_2 forms, respectively, with Δ = 19.1 kcal/mol.

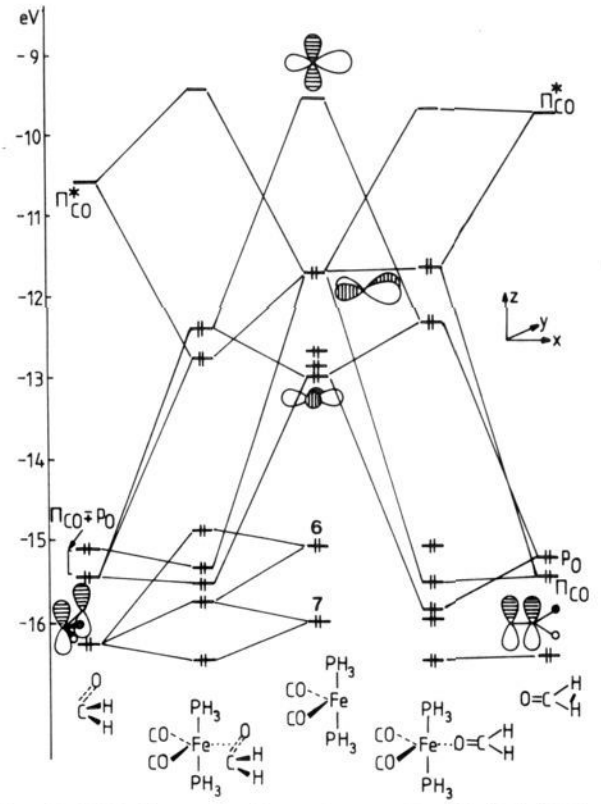

Figure 3. Orbital interaction diagram between the d^8 $Fe(CO)_2(PH_3)_2$ fragment and H_2CO in the η_1 form (on the right) and in the η_2 form (on the left). Orbitals **6** and **7** are drawn in the text.

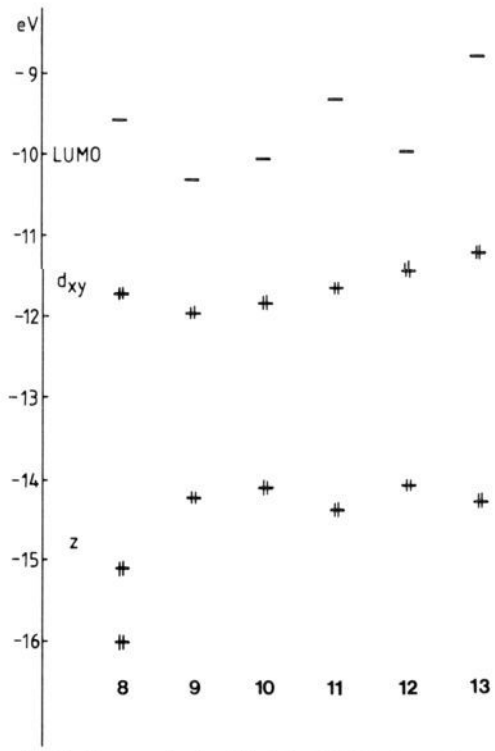

Figure 4. Relative energies (in eV) of the LUMO, d_{xy}, and z orbitals of the d^8 metallic fragments FeL_4 **8** to **13**.

This suggests that in all the examples studied here, only the ones with a small η_1 preference could be modified by such a substitution.

1.2. The d^8 ML_4 Fragment. Five new d^8 ML_4 (**9**–**13**) fragments have been considered and compared with the $Fe(CO)_2(PH_3)_2$

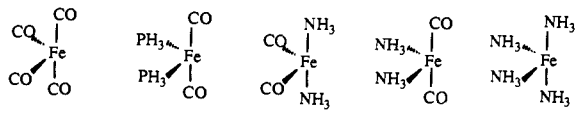

9 10 11 12 13

fragment **8** studied above. The relative energies of the three important orbitals (LUMO, d_{xy}, and z) are plotted in Figure 4. When the axial ligands are CO, the LUMO is an in-phase combination with the π^*_{CO} orbital and is lowered. When the axial ligands are PH_3 or NH_3, the LUMO is an out-of-phase combination with the P or N lone pair and is destabilized, more for NH_3 than for PH_3.

The d_{xy} orbital is an in-phase combination with the π^*_{CO} orbital whether the CO's are equatorial or axial. When the phosphines are axial, they do not give any combination with the HOMO because the p orbitals are too low. When NH_3 ligands are axial, the π_{NH3} orbitals combine slightly with d_{xy} in an out-of-phase way. When PH_3 or NH_3 ligands are equatorial, their lone pairs give an out-of-phase combination with d_{xy} and destabilize it (more NH_3 than PH_3).

Finally, the z orbital is essentially the in-phase combination of the metal p_z orbital and the σ lone pair of CO, PH_3, or NH_3 along the z axis. It is mostly located on the ligands. It is therefore higher with CO than with NH_3, or with PH_3. When the equatorial ligands are CO's, orbital p_z is slightly stabilized (in-phase with π^*_{zCO}). When the equatorial ligands are PH_3 or NH_3 it is, on the contrary, destabilized (out-of-phase combination with π_{PH3} or π_{NH3}). In the case of **8**, this orbital is split into two by mixing with the low-lying π_{CO} orbitals. This is the only case where this happens owing to the low position of the p_z orbital with PH_3 as axial ligands.

Since the vacant p_z orbital of iron and the ligand lone pair are at very different energy, the interaction variation is dominated by the overlap difference when the ligand is changed. The nitrogen or carbon orbitals are more contracted than those of phosphorus. Therefore the mixing is better with PH_3 than with NH_3 or CO, and the coefficient of Fe p_z in the resulting low-lying z orbital is larger for PH_3. As a consequence, the overlap of this orbital with the p_z orbital of R_2CO is also greater for PH_3. Therefore, the four-electron ligand–ligand interactions are stronger with PH_3 since they depend essentially on this overlap.

In summary, axial CO or NH_3 gives less ligand–ligand four-electron interactions than PH_3 and thus favors the η_2 coordination. Furthermore, NH_3 has the greatest effect in destabilizing both d_{xy} and the LUMO, two factors which favor the η_2 coordination. The computational results agree with these assumptions (Table V). The complexes of **11**, **12**, and **13** with H_2CO have not been calculated since it seems obvious that Δ will only be more positive and the complexes remain η_2. On the contrary, their complexes with $(CH_3)_2CO$ or $(CF_3)_2CO$ are interesting since they yield a modification of the coordination mode from η_1 to η_2. The coordination is η_2 for formaldehyde, whatever the metallic fragment, in agreement with the known experimental structures for $Fe(CO)_2(PR_3)_2(H_2CO)$[7] and $Os(CO)_2(PR_3)_2(H_2CO)$.[5]

There are no experimental data for acetone ML_4 complexes. Our calculations suggest that the coordination mode could be metal dependent with a clear tendency for η_1 coordination in the case of $Fe(CO)_2(PR_3)_2(Me_2CO)$ with axial PR_3, which is the most stable conformation. As explained before, this η_1 preference is caused by a strong four-electron repulsion with axial PR_3 for the η_2 coordination and a better electron-donating capability of acetone compared with formaldehyde. On the contrary, the η_2 coordination is more favored for ruthenium or in the case of $M(NH_3)_4$.

An interesting feature is the change in coordination of acetone or hexafluoroacetone with the ruthenium fragment $Ru(CO)_2(PH_3)_2$ when the role of the ligands CO and PH_3 is inverted (axial versus equatorial). With PH_3 axial, the coordination is η_1; with CO axial, it is η_2. This is in agreement with the experimental data; it has been shown by ^{19}F NMR spectroscopy[6a] that the phosphines in $Ru(CO)_2[PEtC(CH_2O)_3]_2$–$\eta_2$-$(CF_3)_2CO$ are in the equatorial plane with axial CO groups.

Table V. Energy Difference Δ (kcal/mol) between the η_1 and η_2 Forms of the $ML_4(R_2CO)$ Complexes Depending on the Metal, the Ligands L, and the Substituents R[a]

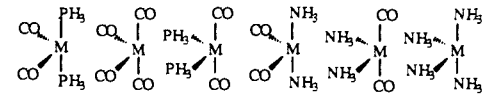

8 9 10 11 12 13

H_2CO	Fe	6.2	9.2	12.6			
	Ru	21.8	20.5	28.3			
$(CH_3)_2CO$	Fe	-27.8	-9.0	-5.3	-4.4	-2.3	12.9
	Ru	-5.7	3.9	12.4	10.1	10.3	23.7
$(CF_3)_2CO$	Fe	-34.9	-8.7	-5.8	-10.8	-1.6	7.8
	Ru	-16.8	8.5	17.3	12	15.2	25.3

[a] A positive value means that the η_2 form is more stable.

Table VI. Energy Difference Δ (kcal/mol) between the η_1 and η_2 Forms of the $ML_5(R_2CO)$ Complexes Depending on the Metal and on the Ligands[a]

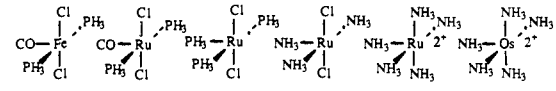

H_2CO	-29.9	-9.2	-4.6	10.8	11.7	19.5
$(CH_3)_2CO$	-59.8	-33.6	-32.0	-8.7	-4.4	2.3

[a] A positive value means that the η_2 form is more stable.

A last comment of Table V concerns the comparison between acetone and hexafluoroacetone. As we said before, the four-electron ligand–ligand interactions are stronger for $(CF_3)_2CO$ than for $(CH_3)_2CO$. Therefore when these interactions predominate, the η_2 coordination is less preferred for hexafluoroacetone than for acetone (case of **8**, **11** (for Fe), **13** (for Fe)). When the two-electron frontier orbital interactions predominate, the inverse is true (case of **9**, **10**, **12**, and **11**, **13** for Ru).

The complexes of Table V with Os replacing Fe or Ru have not been computed except **8** with H_2CO (see above). Since Os is more electropositive than Ru, the η_2 form will be more favored in all osmium complexes than in ruthenium ones.

1.3. The d^8 $C_{2v}ML_3$ and d^6 ML_5 Fragments. The d^6 ML_5 fragment (as, for example, **14**) differs from the d^8 $C_{2v}ML_3$

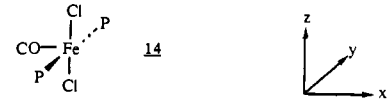

14

fragment by addition of two ligands perpendicular to the ML_3 plane. Its frontier orbitals are similar to those of the d^8 ML_3 fragment (Figure 2) except that d_{z^2} is strongly destabilized. Consequently, the orbital interactions of a d^6 ML_5 fragment with R_2CO are similar to those shown in Figure 2.

The C=O bond in the ML_5 (η_2-R_2CO) complexes is forced to be coplanar with three L ligands independently of the conformation. Such a geometry has been shown to be unfavorable for steric reasons.[19] Therefore, besides electronic factors, these steric constraints will contribute to favor the η_1 coordination.

This suggests that the η_1 coordination with a ML_5 fragment will be more preferred than with a ML_3 fragment. The study of $FeCOCl_2(PH_3)_2(R_2CO)$ and $RuCOCl_2(PH_3)_2(R_2CO)$ confirms this (Table VI). The influence of the metal nature is again pointed out. These results agree with the η_1 experimental structure of $Ru(PH_3)_2COCl(SnCl_3)(CH_3)_2CO$.[9]

Table VII. Energy Difference Δ (kcal/mol) between the η_1 and η_2 Forms of the $CpML_2(R_2CO)$ Complexes[a]

	$CpFe^+(CO)_2$	$CpRe(CO)_2$	$CpRe^+NO(PH_3)$
H_2CO	−7.6	9.2	17.0
$(CH_3)HCO$		−0.7	9.9
$(CH_3)_2CO$	−32.4	−9	−5.5

[a] A positive value means that the η_2 form is more stable.

Let us now look at the influence of the ligand nature. When the ligand along the x axis is CO, orbital d_{xy} is stabilized by in-phase interaction with π^*_{CO}. When it is NH_3, d_{xy} is almost pure without any contribution from the ligand. If CO is replaced by NH_3, d_{xy} shifts up and the η_2 form would be favored. However, the most interacting ligand in the LUMO is also along the x axis (Figure 2). When CO is replaced by NH_3, the out-of-phase combination with σ_{CO} is replaced by that with the N lone pair, which is lower in energy than σ_{CO}. The LUMO is thus less destabilized by NH_3, which favors the η_1 form. Consequently, the replacement of CO by NH_3 induces two opposite effects, one favoring the η_2 form, the other the η_1 form. The former is nevertheless predominant because the interacting orbitals (π^*_{CO} of R_2CO and d_{xy}) are nearer in energy than the oxygen lone pair and the LUMO. A stronger donor ligand, like an alkyl, on the x axis would favor the η_2 form even more. The replacement of PH_3 by NH_3 has a small effect since the contributions of these ligands are small both in d_{xy} and in the LUMO. It has an effect mainly on the four-electron repulsive interactions since NH_3 has been shown previously to give less repulsive interactions than PH_3.

The results for complexes $RuCl_2(NH_3)_3(R_2CO)$ and $Ru^{2+}(NH_3)_5(R_2CO)$ are given in Table VI. In agreement with the previous comments, the η_2 form is much more favored. This shows that the coordination of aldehydes and ketones can be η_2 on a d^6 ML_5 fragment if the ligands are well chosen and if the metal has sufficiently high d orbitals. This is the case for the complex $Os^{2+}(NH_3)_5(R_2CO)$ for which the η_2 form has been computed to be the most stable even with acetone, in agreement with the experimental structure of $Os^{2+}(NH_3)_5(CH_3)_2CO$.[12] This complex therefore no longer appears as an exception in the behavior of $ML_5(R_2CO)$ complexes.

The same arguments are valid for $ML_3(R_2CO)$ complexes. For example, the results of Table IV are inverted for $PdCl_2NH_3(H_2CO)$ and $PdHClNH_3(H_2CO)$ with Cl trans to H_2CO (Δ = +2 and +4 kcal/mol, respectively). Therefore, it would be possible to find η_2 complexes with the ML_3 fragment.

2. The d^6 $CpML_2$ Fragment. The d^6 $CpML_2(R_2CO)$ complexes are interesting since they exist experimentally in both η_1 and η_2 forms depending on the metal and on the organic part R_2CO (see Introduction).

The d^6 $CpML_2$ fragment is similar to the d^6 ML_5 fragment if one makes the isolobal replacement of a Cp^- by three ligands.[23] Therefore, the interaction diagrams between this fragment and R_2CO look like those of the ML_5 and ML_3 fragments although more orbitals are present. Nevertheless, the four-electron repulsive ligand–ligand interactions do no longer exist since there are no vertical ligands. Therefore, the η_1 form will be less favored than for the ML_3 or ML_5 cases. This is confirmed by our calculations on $CpFe^+(CO)_2(H_2CO)$ for which Δ has been found to be −7.6 kcal/mol (see Table VII). Even so, the η_1 form is still preferred with aldehydes or ketones as ligands, in agreement with experimental results ($CpFe^+(CO)_2(R_2CO)$ with R = H or alkyls).[11]

At this point of the discussion it is easy to understand the behavior of the $CpRe(CO)_2$ or $CpRe^+(NO)PH_3$ metallic fragment. Rhenium is a d^7 transition metal of the third line in the periodic table. It is, therefore, an electropositive metal and has d orbitals higher than iron (cf. the set of parameters used by Pyykkö[24]). With the conclusion in mind that the higher the metal orbitals, the more favored the η_2 coordination, one explains that

Scheme II

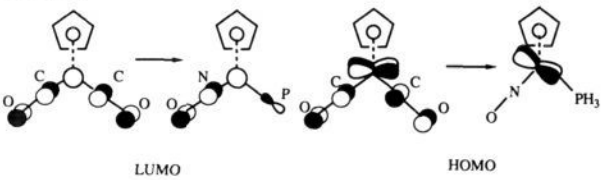

formaldehyde prefers the η_2 coordination on $CpRe(CO)_2$[14b] by comparison with $CpFe^+(CO)_2$. The effect of changing CO with NO or PH_3 in $CpML_2$ fragments already has been well explained:[23b] NO lowers the orbitals and PH_3 shifts them up. In the symmetrical $CpRe^+(CO)_2$ fragment both the LUMO and the HOMO are in-phase combinations with π^*_{CO} of the carbonyls and are thus stabilized. When the CO's are replaced by NO and PH_3, the LUMO does not change a lot; it remains the in-phase combination with π^*_{NO} which is a better π acceptor than CO, but it is also the out-of-phase combination with the lone pair of PH_3. The two effects cancel and the LUMO keeps the same position. On the contrary, the HOMO is strongly destabilized. It loses its bonding character with π^*_{CO} and is now oriented toward PH_3 with no interaction with the ligands (π_{PH_3} is too low in energy). The two orbitals are shown in Scheme II. The result is that the η_1 coordination does not differ between $CpRe^+(CO)_2$ and $CpRe^+(NO)PH_3$. On the contrary, the η_2 coordination is much more favored for the latter. The results of Table VII confirm this analysis.

Experimentally, complex $CpRe^+(NO)PH_3(H_2CO)$ has a long CO bond (1.375 Å instead of 1.32 in usual η_2 complexes). This is a consequence of the high HOMO of $CpRe^+(NO)PH_3$ that induces a large back-donation into the π^*_{CO} orbital of H_2CO. The C–O overlap population is reduced, 0.68 compared to 0.82 in free H_2CO or 0.74 in $Ni(PH_3)_2(H_2CO)$ (see also section III.3).

It has been shown previously that the replacement of H by CH_3 in H_2CO favors the η_1 form relative to the η_2 one. Of course, the effect is smaller if only one H is replaced. Therefore, the behavior of acetaldehyde is intermediate between those of formaldehyde and acetone. The rhenium d orbitals have such a position that the coordination on $CpRe^+(NO)PH_3$ is η_2 for some aldehydes and η_1 for acetone. This fragment is just at the frontier between the two forms so that a small change of the substituents on the aldehydes inverts the coordination. This is illustrated by the study of Gladysz et al. on aromatic aldehydes bearing electron-donating or electron-withdrawing groups.[14c] This is another illustration of the importance of the nature of the ligands for the preferred coordination mode.

3. The d^4 Cp_2 M Fragment. The orbitals of the Cp_2 M fragment have been described previously.[25] For a d^4 complex (M = Mo

or W) they consist of two occupied orbitals $d_{x^2-y^2}$ and d_{xy} (HOMO) and of a LUMO which has an axial symmetry along the x axis. Therefore, the d^4 Cp_2 M fragment has frontier orbitals looking like those of the previously studied fragments and the same arguments will remain valid. Mo and W are early transition metals with high d orbitals. They give rise to a large π^*_{CO}–d_{xy} interaction which favors the η_2 coordination to a great extent. This is verified experimentally; the coordination is η_2 in $Cp_2Mo(H_2CO)$[26] and the C=O distance is long (1.36 Å).

A related complex is $Cp_2V(H_2CO)$[27] where the coordination is also η_2. The metallic fragment is d^3 and the HOMO d_{xy} is singly occupied. Owing to the high position of the vanadium d orbitals, a greater stabilization is obtained in the η_2 form with the one-electron HOMO–π^*_{CO} interaction than in the η_1 form with the

(23) (a) Shilling, B. E. R.; Hoffmann, R.; Lichtenberger, D. L. *J. Am. Chem. Soc.* **1979**, *101*, 585. (b) Shilling, B. E. R.; Hoffmann, R.; Faller, J. W. *J. Am. Chem. Soc.* **1979**, *101*, 592.

(24) (a) Rösch, N. QCPE 468, *QCPE Bull.* **1983**, *3*, 105. (b) Rohr, L. L., Jr.; Hotokka, M.; Pyykkö, P. *QCPE* **1980**, *12*, 387.

(25) Lauher, J. W.; Hoffmann, R. *J. Am. Chem. Soc.* **1976**, *98*, 1729.

(26) Gambarotta, S.; Floriani, C.; Chiesi-Villa, A.; Guastini, C. *J. Am. Chem. Soc.* **1985**, *107*, 2985.

(27) Gambarotta, S.; Floriani, C.; Chiesi-Villa, A.; Guastini, C. *Organometallics* **1986**, *5*, 2425.

two-electron LUMO–oxygen lone pair interaction. Effectively, the C=O bond is long, 1.353 Å. This system is interesting because it gives an η_1 complex when the oxidation state of the metal changes. For example, complex $Cp_2V^+(CH_3)_2CO$ has been isolated in the η_1 form.[28] This is easy to understand since the d_{xy} orbital which interacted with π^*_{CO} is now empty. The back-bonding interaction which favors the η_2 form no longer exists and only the η_1 form becomes possible.

V. Conclusion

The extended Hückel calculations performed in this work provide a good rationalization of the coordination mode of aldehydes and ketones on metallic fragments. The interaction between the hydrocarbon fragment and the organometallic center can be divided into two components. There are first the well-known two-electron frontier orbital interactions which clearly distinguish the η_1 and η_2 forms: the oxygen lone pair – LUMO of the complex interaction in the η_1 form and the π^*_{CO}–d occupied orbital interactions in the η_2 form. It is obvious from overlap and energy criteria that this two-electron interaction is generally stronger in the case of the lateral η_2 coordination.

The higher the metal d orbitals (more electropositive metal), the more favored is the η_2 form compared with the η_1 form. On the other hand, higher orbitals on the organic part (donor substituents on formaldehyde) would favor the η_1 form with respect to the η_2 one.

However, the description of the electronic structure of the complexes cannot be limited in all cases to the frontier orbital approximation. Four-electron interactions between low-lying orbitals centered on the ligands play an important role in the determination of the preferred structure. Occupied orbitals of the organic molecule feel a repulsion from electrons of other ligands on the complex such as chlorine or phosphine. This repulsion is not simply a steric effect which would result from a direct through-space overlap of the ligands but it is caused by simultaneous overlap of two ligands of the complex with the same d orbital on the metal.

If the η_2 coordination for the $Ni(PH_3)_2$ fragment is primarily explained by the frontier orbital interactions, these ligand–ligand indirect couplings are crucial for the analysis of the η_1 preferred mode in the case of $NiCl_2(PH_3)$. They would also favor a η_1 coordination for $Fe(CO)_2(PH_3)_2$ but are not strong enough to compensate a large tendency toward η_2 caused by the two-electron interactions.

For the d^8 ML_4 and d^6 ML_5 (or equivalently d^6 $CpML_2$) fragments, both η_1 or η_2 coordinations could be found depending on the nature of the metal and ligands. This control of the coordination by the organometallic fragment has been detailed and allows an understanding of the various experimental structures. It is especially effective in the case of the d^6 $CpML_2$ fragment which lies at the border line between η_1 and η_2 preference and then can be easily displaced from one form to the other.

Appendix I

All calculations were performed by using the extended Hückel method[29] with weighted H_{ij}'s. The values for the H_{ii}'s and exponents are taken from previous work: ref 30 for Ni, Pd, Pt, and Fe; ref 31 for Ru and Os. They do not include relativistic corrections.

Appendix II. Geometry of the Studied Complexes

The method used does not allow a fully geometry optimization especially for the bond lengths. On the contrary, it often gives good angles because they are related to the orientation of orbitals. Therefore, in most cases, bond lengths have been the experimental ones.

The CO bond lengths were 1.22 Å (η_1) and 1.32 Å (η_2) for formaldehyde, 1.24 Å (η_1) and 1.34 Å (η_2) for ketones. In all cases the M–C bond has been taken to be 0.03 Å longer than the M–O bond for which the same value has been chosen in both the η_1 and the η_2 forms: Ni–O, 1.9 Å; Pd–O or Pt–O, 1.98 Å; Fe–O, 2 Å; Ru–O, 2.19 Å.

Some features are general for all complexes. First, the carbon is pyramidalized in the η_2 form as it is found experimentally.[4b,12a] The same geometry is found in olefin complexes and for the same electronic reasons[19] (lowering of π^*_{CO} and hybridization toward the metallic fragment). Secondly, in all known η_1 complexes the metal–O–C angle varies between 130° and 150°. From our calculations it appears that the energy decreases slightly when this angle is varied from 120° to 145° (4 kcal/mol); then the variation is quasi-null. This could signify that there exists a flexibility in the movement of the R_2CO part in solution, the bent conformation in the crystalline form resulting from constraints. This assumption is supported by the NMR measurements of $PtCl_2(pyr)(CH_3)_2CO$[8a] in solution, which show a coalescence phenomenon of the methyl signals, or of $CpFe^+(CO)_2(R_2CO)$.[11] We have always considered the linear form. The rotation of CH_2 around the metal–O bond needs only 1 to 2 kcal/mol. There is free rotation as in the Pt complex.[8a]

Let us consider now the metallic fragments successively. In the $ML_2(\eta_2\text{-}R_2CO)$ and $ML_4(\eta_2\text{-}R_2CO)$ complexes, the C=O bond has been found to lie in the xy plane in agreement with the geometries of olefin complexes.[19] The LML angle in the xy plane has been called θ. For the ML_2 fragment, the optimization of θ gives a value of 130° in the η_1 form and 115° in the η_2 form (experimental value 106–108°[4]). For the ML_4 fragment, θ has been computed to be 140° in the η_1 form. The situation is more complicated in the η_2 form. With H_2CO or $(CH_3)_2CO$ as ligand, the best value of θ is 105° in agreement with the experimental value (103°).[7] The pyramidalization angle at C is greater than for $ML_2(R_2CO)$ complexes (45–50° instead of 40°). With $(CF_3)_2CO$ as ligand, the C_{2v} geometry of the $M(PH_3)_2(CO)_2$ fragment is not kept and is replaced by a C_{4v} one as shown in **15** with α = 105°.

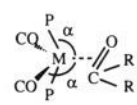

15

Such a geometry agrees with Hoffmann's calculations:[32] "for the d^8 ML_5 complex the trigonal bipyramid is the most stable, but the square-pyramidal geometry with α = 105° is not far above in energy". A special case of ML_4 fragment appears when two NH_3 ligands are equatorial (for example, **12** or **13**). In the η_1 form the geometry is C_{4v} with α = 95°; the η_2 form has always a C_{2v} geometry but θ is smaller (θ = 90°).

For the $ML_3(\eta_2\text{-}R_2CO)$ complexes, the best conformation has the C=O bond perpendicular to the ML_3 plane, as in the ML_3 complexes of ethylene.[19] The in-plane conformation is far above (41 kcal/mol), and the reason is essentially steric (too short distances between C, O, and L).

In the $ML_5(\eta_2\text{-}R_2CO)$ complexes, the C=O bond is forced to be in-plane with three ligands. The steric constraints can be released by bending back (5°) the in-plane ligands away from the C=O bond. The same determination has been made by Hoffmann[19] and is verified experimentally in $Os^{2+}(NH_3)_5\text{-}\eta_2\text{-}(CH_3)_2CO$.[12] In the $MCOCl_2(PH_3)_2(\eta_2\text{-}R_2CO)$ complexes, R_2CO prefers to be parallel to the PH_3 ligands rather than to the Cl ligands. Two reasons explain that. Firstly the π^*_{CO} orbital of R_2CO overlaps with d_{xy} in one case, with d_{xz} in the other case.

In d_{xy} only the CO ligand plays a role. In d_{xz} the chlorines also

(28) Gambarotta, S.; Pasquali, M.; Floriani, C.; Chiesi-Villa, A.; Guastini, C. *Inorg. Chem.* **1981**, *20*, 1173.
(29) Hoffmann, R. *J. Chem. Phys.* **1963**, *24*, 1397.
(30) Eisenstein, O.; Hoffmann, R. *J. Am. Chem. Soc.* **1981**, *103*, 4308.
(31) Fu-Tai Tuan, D.; Hoffmann, R. *Inorg. Chem.* **1985**, *24*, 871.
(32) Elian, M.; Hoffmann, R. *Inorg. Chem.* **1975**, *14*, 1058.

have an important interaction so that d_{xz} is more delocalized on the ligands than d_{xy} and has a smaller overlap with π^*_{CO} of R_2CO. Secondly the ligand–ligand 4e repulsive interactions are stronger for PH_3 than for Cl.

Finally, in $CpM(CO)_2(\eta_2\text{-}R_2CO)$ complexes, the C=O bond bisects the molecular mirror plane as in ethylene complexes.[23] The CO's must be bent back by 10° in order to remove the steric hindrance between C and the CO ligand (C–C overlap population of 0.08). For the $CpRe^+(NO)PH_3(R_2CO)$ complexes, the experimental geometry has been taken both in the η_1[13] and η_2[14a] forms. The orientation of R_2CO is such that the π^*_{CO} orbital overlaps with the HOMO of the metallic part (see Scheme II).

Photosynthetic Water Oxidation Center: Spin Frustration in Distorted Cubane $Mn^{IV}Mn^{III}_3$ Model Complexes

David N. Hendrickson,*[1a] George Christou,*[2a] Edward A. Schmitt,[1a] Eduardo Libby,[2a] John S. Bashkin,[2a] Sheyi Wang,[2a] Hui-Lien Tsai,[1a] John B. Vincent,[2a] Peter D. W. Boyd,[3] John C. Huffman,[2b] Kirsten Folting,[2b] Qiaoying Li,[1b] and William E. Streib[2b]

Contribution from the Department of Chemistry-0506, University of California at San Diego, La Jolla, California 92093-0506, and the Department of Chemistry and the Molecular Structure Center, Indiana University, Bloomington, Indiana 47405. *Received August 14, 1991*

Abstract: Four $Mn^{IV}Mn_3^{III}$ complexes have been prepared as model complexes for the S_2 state of the water oxidation center (WOC) in photosystem II. All of these complexes are prepared by the reaction of a μ_3-oxide Mn_3^{III} complex with Me_3SiCl which leads to a disproportionation to give the $Mn^{IV}Mn_3^{III}$ complex and an Mn^{II} product. The reaction of $Mn(O_2CCH_3)_3\cdot 2H_2O$ with Me_3SiCl followed by addition of imidazole gives $(H_2Im)_2[Mn_4O_3Cl_6(O_2CCH_3)_3(HIm)]\cdot{}^3/_2CH_3CN$ (**1**) where H_2Im^+ is the imidazolium cation. Reaction of $[Mn_3O(O_2CCH_3)_6(py)_3](ClO_4)$ or $[Mn_3O(O_2CCH_2CH_3)_6(py)_3](ClO_4)$ with Me_3SiCl leads, respectively, to $[Mn_4O_3Cl_4(O_2CCH_3)_3(py)_3]\cdot{}^3/_2CH_3CN$ (**2**) and $[Mn_4O_3Cl_4(O_2CCH_2CH_3)_3(py)_3]\cdot{}^5/_2CH_3CN$ (**4**). A similar procedure as for **2** but followed by addition of imidazole yields $[Mn_4O_3Cl_4(O_2CCH_3)_3(HIm)_3]\cdot{}^5/_2CH_3CN$ (**5**). Complex **1** crystallizes in the orthorhombic space group *Pbca* with (at −158 °C) a = 14.307 (14) Å, b = 14.668 (14) Å, c = 31.319 (36) Å, V = 6572.75 Å^3, and Z = 8. A total of 2513 unique data with $F > 2.33\sigma(F)$ were refined to values of R and R_w of 8.10 and 8.70%, respectively. The central $[Mn_4(\mu_3\text{-}O)_3(\mu_3\text{-}Cl)]^{6+}$ core of the anion in complex **1** consists of a Mn_4 pyramid with the Mn^{IV} ion at the apex, a μ_3-Cl^- ion bridging the basal plane, and a μ_3-O^{2-} ion bridging each of the remaining three faces. The Mn^{IV} ion has six oxygen atom ligands, three from the three μ_3-O^{2-} ions and three from the bridging acetates. Two of the Mn^{III} ions have $Mn(Cl)_2(\mu_3\text{-}Cl)(\mu_3\text{-}O)_2(\mu\text{-}O_2CCH_3)$ coordination spheres; the third Mn^{III} ion has one of the terminal Cl^- ligands replaced by an imidazole ligand. The complex $[Mn_4O_3Cl_4(O_2CCH_3)_3(py)_3]\cdot{}^3/_2CH_3CN$ (**2**) crystallizes in the hexagonal space group $R\bar{3}$ with (at −155 °C) $a = b = c$ = 13.031 (4) Å, $\alpha = \beta = \gamma$ = 74.81 (2)°, V = 2015.93 Å^3, and Z = 2. A total of 1458 unique data with $F > 3.0\sigma(F)$ were refined to values of R and R_w of 3.71 and 4.17%, respectively. The $Mn^{IV}Mn_3^{III}O_3Cl$ core in complex **2** is essentially superimposable with that of complex **1**. Complex **2** has crystallographically imposed C_3 symmetry. The other two complexes, $[Mn_4O_3Cl_4(O_2CCH_2CH_3)_3(py)_3]\cdot{}^5/_2CH_3CN$ (**4**) and $[Mn_4O_3Cl_4(O_2CCH_3)_3(HIm)_3]\cdot{}^5/_2CH_3CN$ (**5**), also crystallize in the $R\bar{3}$ space group. The unit cell of complex **4** has (at −143 °C) $a = b = c$ = 13.156 (6) Å, $\alpha = \beta = \gamma$ = 74.56 (3)°, V = 2068.53 Å^3, and Z = 2. A total of 1425 unique data with $F > 3.0\sigma(F)$ were refined to values of R and R_w of 5.265 and 5.44%, respectively. The unit cell of complex **5** has (at −145 °C) $a = b$ = 15.656 (6) Å, c = 26.947 (9) Å, $\alpha = \beta$ = 90°, γ = 120.0°, V = 5722.68 Å^3, and Z = 6. A total of 1156 unique data with $F > 3.0\sigma(F)$ was refined to values of R and R_w of 5.75 and 5.90%, respectively. The $Mn^{IV}Mn_3^{III}O_3Cl$ core of these complexes is compared with the core of S_1-state model complexes which have the $Mn_4^{III}(\mu_3\text{-}O)_2$ butterfly structure. It is suggested that increasing the oxidation state from S_1 to S_2 state is coupled to an increase in oxide content. A strong Mn–O stretching IR band at 580–590 cm^{-1} is identified as characteristic of $Mn^{IV}Mn_3^{III}O_3Cl$ cubane complexes. No reversible waves were observed in the electrochemistry of these complexes. However, ^{1}H NMR and Beers law dependence studies show that complex **1** remains intact in DMF as do complexes **2** and **4** in CH_2Cl_2 and $CHCl_3$. Magnetic susceptibility data are presented for complexes **1**, **2**, and **4** at 10.0 kG in the 5–300 K range. The value of μ_{eff}/molecule at room temperature increases with decreasing temperature to give a maximum at 60 K for **1** and **2** and 15 K for **4**. Below these temperatures μ_{eff}/molecule drops relatively abruptly. The data were fit to a theoretical model to give exchange parameters $J_{34}(Mn^{IV}\cdots Mn^{III})$ of −20.8 to −30.3 cm^{-1} and J_{33} of +8.6 to 11.3 cm^{-1}. The ground state for all complexes is a well-isolated $S_T = {}^9/_2$ state. This was confirmed by variable field magnetization studies: ~2–40 K at fields of 24.8, 34.5, and 44.0 kG for complex **2**; ~2–15 K at fields of 10.0, 30.0, and 48.0 kG for complex **4**. These data were fit by a matrix diagonalization approach with Zeeman and axial zero-field ($D\hat{S}_z^2$) interactions to verify a $S_T = {}^9/_2$ ground state with $D \simeq +0.3$ cm^{-1}. The nature of the spin frustration in these $Mn^{IV}Mn_3^{III}O_3Cl$ cubane complexes is analyzed in detail. It is shown what other ground states may be possible for such a complex. Variable-temperature X-band EPR data are presented for polycrystalline and frozen glass samples of complexes **1**, **2**, and **4**. Q-band spectra are also given for solid samples. A detailed map of expected X-band resonance fields plotted versus the axial zero-field splitting parameter is derived for a complex with $S_T = {}^9/_2$ ground state. The experimental EPR spectra are shown to be qualitatively in agreement with these calculated resonance fields. The electronic structure of the four $Mn^{IV}Mn_3^{III}O_3Cl$ cubane complexes is discussed with the goal of modeling the S_2 state of the WOC.

Introduction

Polynuclear metal complexes are found as the active sites in several metalloproteins. The electronic structures of many of these polynuclear active sites are complicated, and, as a consequence, there is a sensitivity to extrinsic factors. Recent work[4,5] on $[Fe_4S_4(SR)_4]^{3-}$ complexes which mimic the active sites in certain electron transport proteins has established that these complexes

(1) (a) University of California at San Diego. (b) Present address: University of California at Santa Barbara.
(2) (a) Department of Chemistry, Indiana University. (b) Molecular Structure Center, Indiana University.
(3) On sabbatical leave from the University of Auckland, Auckland, New Zealand.

(4) Carney, M. J.; Papaefthymiou, G. C.; Spartalian, K.; Frankel, R. B.; Holm, R. H. *J. Am. Chem. Soc.* **1988**, *110*, 6084–6095, and references therein.
(5) Carney, M. J.; Papaefthymiou, G. C.; Whitener, M. A.; Spartalian, K.; Frankel, R. B.; Holm, R. H. *Inorg. Chem.* **1988**, *27*, 346–352.

0002-7863/92/1514-2455$03.00/0